

# Microstructural Development during Liquid-phase Sintering of $\text{Si}_3\text{N}_4$ Ceramics

C. Boberski, H. Bestgen, R. Hamminger

Hoechst AG, Postfach 80 03 20, 6230 Frankfurt am Main 80, FRG

(Received 6 May 1991; accepted 20 June 1991)

## Abstract

*The intermediate states of liquid-phase sintering of silicon nitride with 10.01 wt.%  $\text{Y}_2\text{O}_3$  and 2.28 wt.%  $\text{Al}_2\text{O}_3$  were studied with dilatometer equipment concerning the phase contents and the microstructural development. The phase transformation of  $\text{Si}_3\text{N}_4$  from  $\alpha$  to  $\beta$  starts when the liquid phase appears and is completed after full densification. The sub-solidus reaction, melting of the sintering additives and the distribution of the glassy phase during sintering were investigated by analytical transmission electron microscopy.*

*Das Sinterverhalten während des Flüssigphasensinterns von Siliziumnitrid mit 10.01 Gew.%  $\text{Y}_2\text{O}_3$  und 2.28 Gew.%  $\text{Al}_2\text{O}_3$  wird in einem Hochtemperatur-Dilatometer untersucht. Die unterschiedlichen Sinterstadien werden durch das Gefüge und die Phasenzusammensetzung charakterisiert. Die Phasenumwandlung von  $\alpha\text{-Si}_3\text{N}_4$  zur  $\beta$ -Modifikation beginnt, wenn die flüssige Glasphase gebildet wird, und ist nach der vollständigen Verdichtung abgeschlossen. Die Reaktion der Additive miteinander sowie die beginnende Aufschmelzung der Additive und deren Verteilung in der Probe werden mit Hilfe eines analytischen Transmissionselektronenmikroskops verfolgt.*

*Les états intermédiaires du frittage en phase liquide du nitrure de silicium contenant 10.01 wt% de  $\text{Y}_2\text{O}_3$  et 2.28 wt% d' $\text{Al}_2\text{O}_3$  ont été étudiés avec un dilatomètre en ce qui concerne la composition des différentes phases et l'évolution de la microstructure. La transformation du  $\text{Si}_3\text{N}_4$  de la phase  $\alpha$  à la phase  $\beta$  commence lorsque la phase liquide apparaît et se termine après densification totale. La réaction sub-*

*solide et la liquéfaction des additifs de frittage ainsi que la distribution de la phase vitreuse pendant le frittage ont été analysée au moyen d'un microscope électronique à transmission.*

## 1 Introduction

$\text{Si}_3\text{N}_4$  cannot be densified in the conventional way without the addition of sintering aids. By adding e.g.  $\text{Al}_2\text{O}_3$  and  $\text{Y}_2\text{O}_3$ , liquid-phase sintering is initiated, producing dense ceramic bodies. Densification is strongly affected by the purity and fineness of the initial powders, processing methods, type and amount of sintering aids, the sintering parameters. The resulting microstructure of  $\text{Si}_3\text{N}_4$ , i.e. the grain morphology, the intergranular phase and the residual porosity, determines the mechanical strength. On cooling the liquid phase forms an intergranular glassy phase that reduces the strength of  $\text{Si}_3\text{N}_4$  above 1000°C (i.e. above the glass softening temperature). Below the glass softening temperature high strength values are obtained with the grain morphology that consists of elongated  $\beta\text{-Si}_3\text{N}_4$  grains with high aspect ratios. It was found that these prismatic grains develop when the liquid phase has a high viscosity, which on the other hand opposes the densification process.<sup>1</sup> In order to optimize the microstructure with respect to the mechanical properties, an understanding of the microstructural development during sintering may be helpful. In this paper microstructural features at various stages of the sintering process are described and discussed in terms of Kingery's<sup>2</sup> sintering model in which three distinct, possibly overlapping stages, particle rearrangement, solution–reprecipitation and coalescence, are treated theoretically.

## 2 Experimental

$\text{Si}_3\text{N}_4$  powder (TS-10, Tosoh, Tokyo, Japan) with 10.01 wt.%  $\text{Y}_2\text{O}_3$  (Ventron, Karlsruhe, FRG) and 2.28 wt.%  $\text{Al}_2\text{O}_3$  (A-16, Alcoa, Bauxite, USA) was milled in an attritor with isopropanol as a solvent, dried, cold isostatic pressed and pressureless sintered for 1 h at 1800°C. The heating rate was 30°C/min. The sintering experiments were carried out in a graphite heated dilatometer to monitor the shrinkage rate at given temperatures. The samples (diameter = 1 cm, height = 1 cm) were placed in a BN crucible. The small graphite heating elements allowed very fast cooling of the samples, making it possible to detect well-defined intermediate states of microstructural development at different temperatures (see Table 1).

The phase content of the quenched samples was determined by X-ray diffraction using  $\text{CuK}_\alpha$ -radiation. The microstructure was characterized using analytical transmission electron microscopy at 300 keV in a Philips CM 30 STEM, fitted with an EDAX energy dispersive X-ray system and a Gatan 666 PEELS spectrometer. Thin foils for STEM were mechanically ground, dimpled to a thickness of about 60  $\mu\text{m}$  and then ion-beam thinned with 6 keV argon ions until perforation.

## 3 Results

The shrinkage and the shrinkage velocity of the samples are shown in Fig. 1(a) and (b), respectively. The shrinkage velocity is characterized by two maxima at 1389°C and at 1615°C, at which latter temperature the major shrinkage takes place. After completion of sintering the total amount of shrinkage was 18% (Fig. 1(a)) and the density 98.5% of

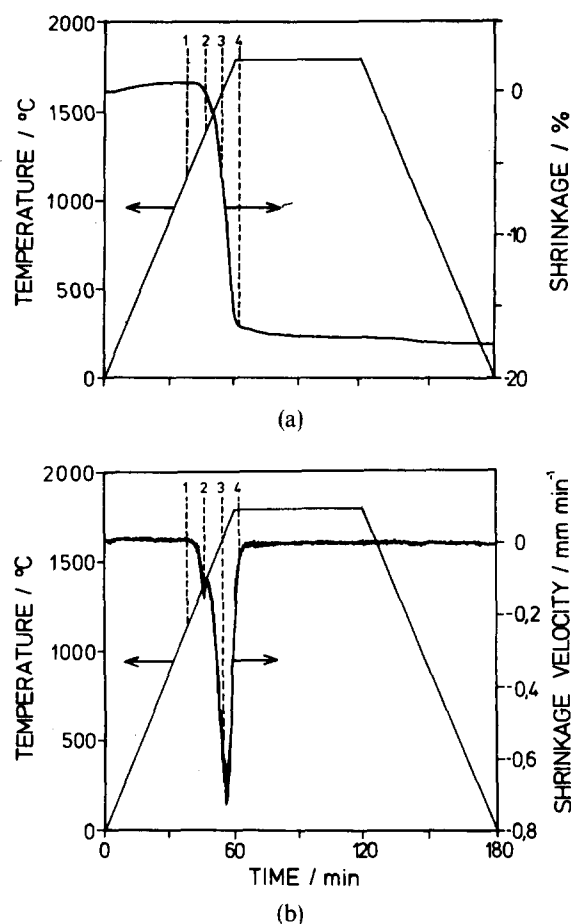


Fig. 1. Pressureless sintering of  $\text{Si}_3\text{N}_4$  with 10.01 wt.%  $\text{Y}_2\text{O}_3$  and 2.28 wt.%  $\text{Al}_2\text{O}_3$ . The shrinkage (a) and the shrinkage velocity (b) are given with the quenching temperatures of the samples. 1, 1139°C; 2, 1389°C; 3, 1615°C; 4, 1800°C.

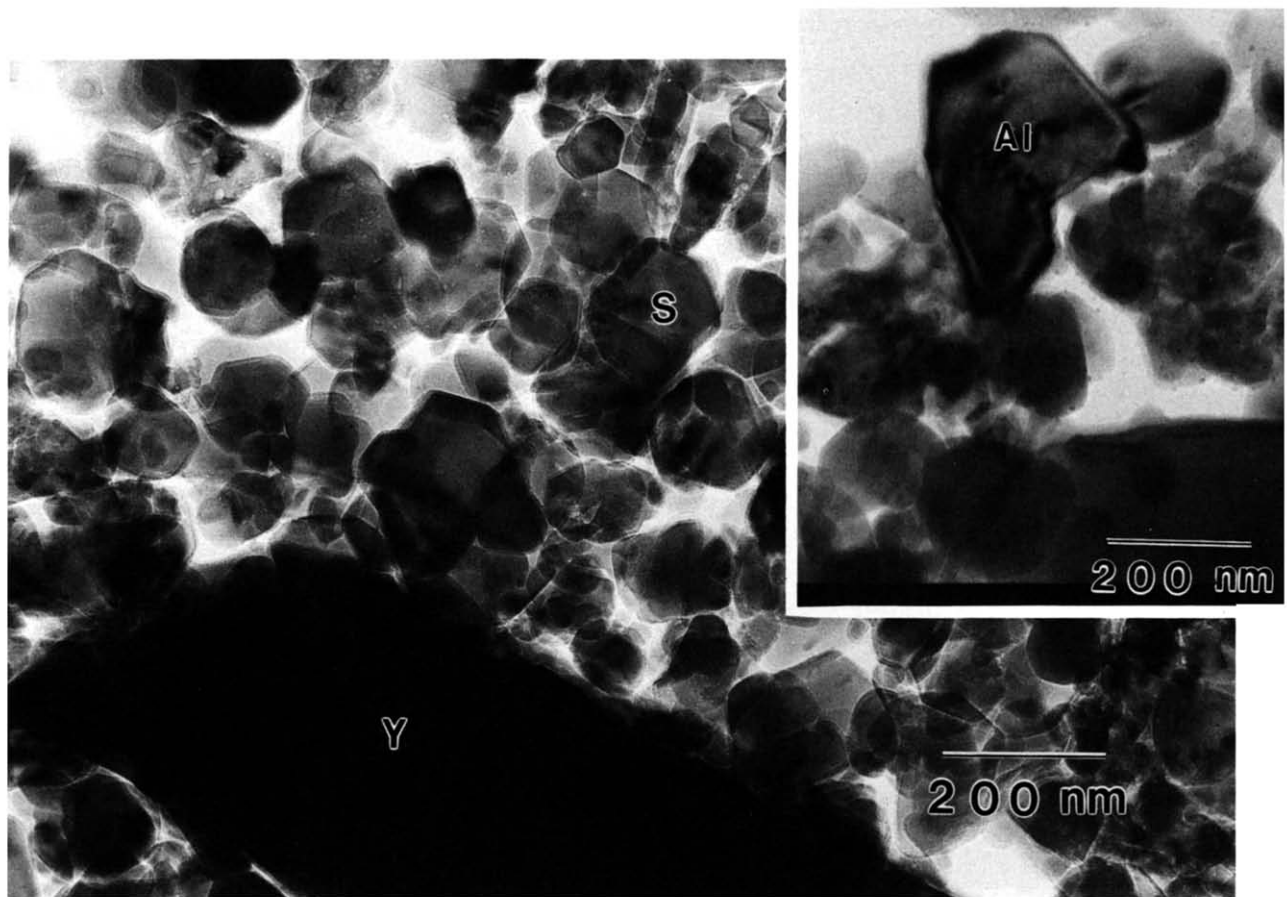
the theoretical value. Samples quenched at 1139°C, 1389°C (first maximum of shrinkage velocity), 1615°C (second maximum of shrinkage velocity) and 1800°C (after completion of shrinkage) were examined (Fig. 1(b)). The phase contents of the samples are listed in Table 1.

The microstructure of the sample quenched at 1139°C is shown in Fig. 2(a). It consists of nearly equiaxed  $\text{Si}_3\text{N}_4$  grains with a particle size between 0.1 and 0.2  $\mu\text{m}$ ,  $\text{Al}_2\text{O}_3$  grains of about 0.5  $\mu\text{m}$ , and  $\text{Y}_2\text{O}_3$  agglomerates of 0.5–1.0  $\mu\text{m}$ . The TEM micrograph of the sample quenched at 1389°C demonstrates the evolution of the microstructure (Fig. 2(b)). The  $\alpha$ - $\text{Si}_3\text{N}_4$  grains are now completely covered by a glassy layer of a thickness of about 10–20 nm, and the porosity has changed from an open to a nearly closed one. Obviously close to the first maximum of the shrinkage velocity, the liquid phase has formed. Assuming an oxide glass, the layer consists of  $\text{Al}_2\text{O}_3$  (2–4 wt%),  $\text{Y}_2\text{O}_3$  (3–5 wt%) and  $\text{SiO}_2$  (91–95 wt%), which was measured at different areas of the sample by EDX analysis. Several of the polycrystalline  $\text{Y}_2\text{O}_3$  particles are not completely dissolved and are

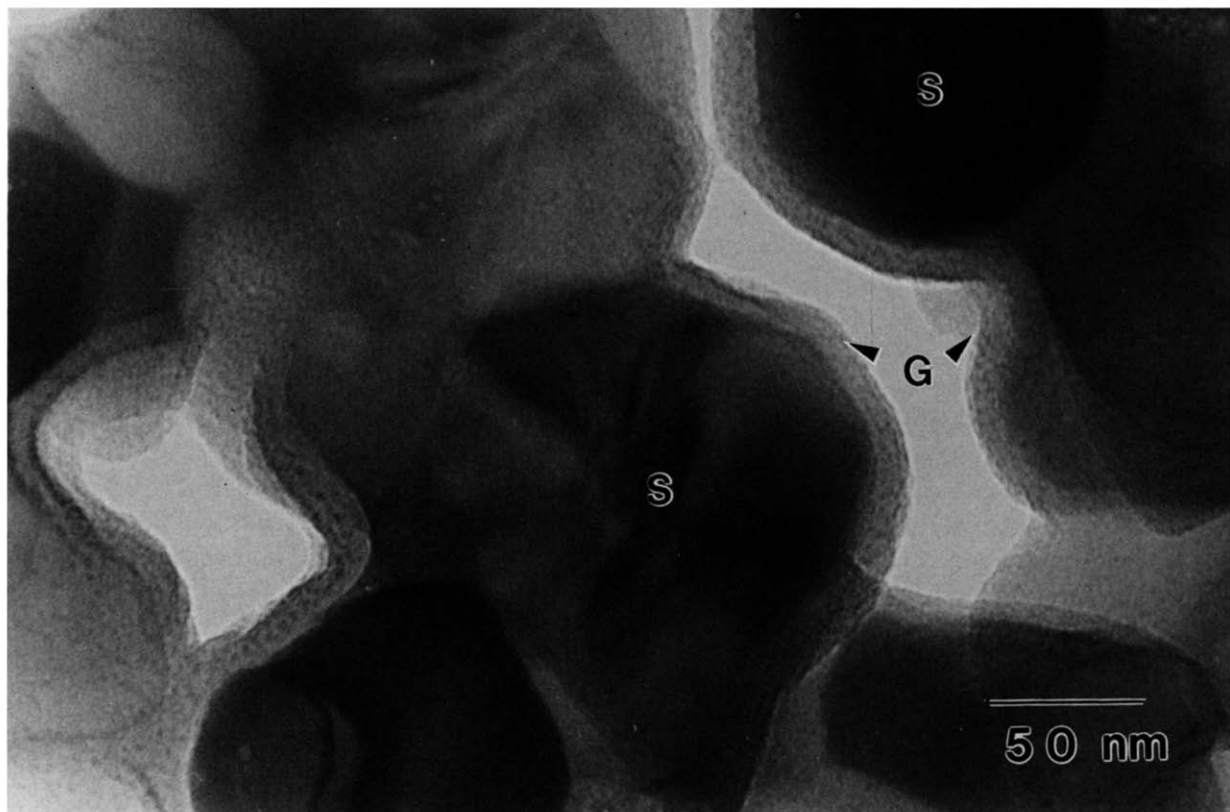
Table 1. Phase contents of the samples quenched at different temperatures

Temperature (°C)	Remark	Phase content
1139	Before shrinkage was measured	$(\alpha/\alpha + \beta)^a = 0.96$ , $\alpha$ - $\text{Si}_3\text{N}_4$ , $\beta$ - $\text{Si}_3\text{N}_4$ , $\text{Y}_2\text{O}_3$ , $\alpha$ - $\text{Al}_2\text{O}_3$ , amorphous
1389	First maximum of shrinkage velocity	$(\alpha/\alpha + \beta) = 0.96$ , $\text{Y}_2\text{SiO}_5$ , amorphous
1615	Second maximum of shrinkage velocity	$(\alpha/\alpha + \beta) = 0.90$ , $\text{Y}_2\text{SiO}_5$ , amorphous
1800°C/2 min	After shrinkage	$(\alpha/\alpha + \beta) = 0.27$ , amorphous

<sup>a</sup> $(\alpha/\alpha + \beta)$ : ratio for  $\alpha$ - and  $\beta$ - $\text{Si}_3\text{N}_4$  determined by X-ray diffraction analysis.<sup>6</sup>



(a)



(b)

**Fig. 2.** Microstructure of the intermediate sintering state. TEM bright field image of  $\text{Si}_3\text{N}_4$  quenched at (a) 1139°C, (b) 1389°C and (c) 1615°C. S,  $\alpha\text{-Si}_3\text{N}_4$ ; Y,  $\text{Y}_2\text{O}_3$ ; Al,  $\text{Al}_2\text{O}_3$ ; G, glassy layer; A,  $\alpha\text{-Si}_3\text{N}_4$  matrix; B,  $\beta\text{-Si}_3\text{N}_4$ .



(c)

Fig. 2—contd.

in a stage of particle disintegration, the melt having penetrated along the grain boundaries. In many  $\alpha$ - $\text{Si}_3\text{N}_4$  grains antiphase boundaries are observed. The size and the shape of the  $\alpha$ - $\text{Si}_3\text{N}_4$  grains are still comparable to those of the sample quenched at 1139°C. The further development of the microstructure is shown in the TEM bright field image of Fig. 2(c). The image shows a  $\beta$ - $\text{Si}_3\text{N}_4$  grain, which is obviously in a growth stage, surrounded by  $\text{Si}_3\text{N}_4$  grains, most of which are smaller than 100 nm. These small, well-rounded grains which are separated by a thin amorphous layer, dominate the microstructure and are still in the  $\alpha$ -phase according to the X-ray measurements. The majority of the  $\beta$ - $\text{Si}_3\text{N}_4$  grains are not prismatic and have curved growth fronts similar to that shown in Fig. 2(c). Several partially grown  $\beta$ - $\text{Si}_3\text{N}_4$  grains consist of subgrains with dislocations in the interfaces. In contrast to this morphology, completely grown  $\text{Si}_3\text{N}_4$  crystals with well-defined crystallographic shapes are observed in the sample quenched at 1800°C (holding time at 1800°C, 2 min), when densification is nearly complete. The intergranular phase is an oxynitride glass which was detected by EELS, and has an  $\text{Al}_2\text{O}_3/\text{Y}_2\text{O}_3$  ratio of 0.17 (in wt.%; determined by

EDX analysis) which is close to that of the starting mixture ( $\text{Al}_2\text{O}_3/\text{Y}_2\text{O}_3 = 0.23$ ).

#### 4 Discussion

From STEM and X-ray analysis of the microstructures of quenched intermediate sintering states, it is evident that the first maximum of the shrinkage velocity at 1389°C correlates with the formation of a liquid phase that wets most of the  $\alpha$ - $\text{Si}_3\text{N}_4$  particles. The second maximum at 1615°C correlates with the phase transformation  $\alpha$ - to  $\beta$ - $\text{Si}_3\text{N}_4$ . The melt forms as the sintering aids react with the  $\text{SiO}_2$  layer covering  $\text{Si}_3\text{N}_4$  (in the system  $\text{Y}_2\text{O}_3$ - $\text{SiO}_2$ - $\text{Al}_2\text{O}_3$  the eutectic temperature is at 1345°C<sup>3</sup>). A comparison of the  $\text{Al}_2\text{O}_3/\text{Y}_2\text{O}_3$  ratio in the starting mixture and in the glassy layer indicates a preferred dissolution of  $\text{Al}_2\text{O}_3$ . The wetting of the  $\text{Si}_3\text{N}_4$  grains by the melt is responsible for primary particle rearrangement being the first step of the densification process.<sup>2</sup> Although this state is often discussed in literature, direct evidence of the wetted  $\text{Si}_3\text{N}_4$  grains in the quenched state, an example of which is shown in Fig. 2(b), is scarce. Studies of the thickness

and the composition of this glassy layer for different types of sintering aids and  $\text{Si}_3\text{N}_4$  powders may yield useful information about reactions between the different components at the beginning of the densification process. The microstructure of the sample quenched at  $1615^\circ\text{C}$  (Fig. 2(c)) is a result of the second and third step of liquid-phase sintering, i.e. solution–reprecipitation and coalescence. While the size of the  $\alpha\text{-Si}_3\text{N}_4$  grains is between 100 and 200 nm before shrinkage, at  $1189^\circ\text{C}$  most of them are now smaller than 100 nm. Therefore, obviously the  $\alpha\text{-Si}_3\text{N}_4$  grains are dissolving, enriching the melt with Si and N. The dissolution of particles is an additional mechanism for rearrangement (secondary rearrangement) which leads to better space filling and an increase in density. Another feature of this specimen is that large areas of the intergranular phase of a size of about 50–100 nm, which are frequently observed in samples cooled after complete densification, are rare.

The fine distribution of the very thin intergranular glassy layer confirms the assumption, made in modelling the solution–reprecipitation process (e.g. Ref. 4), that the liquid interface between the dissolving  $\alpha\text{-Si}_3\text{N}_4$  and the growing  $\beta\text{-Si}_3\text{N}_4$  particles is smaller than a few nanometres. Therefore it is likely that the rate-controlling step for the growth of  $\beta$ -crystals is not diffusion through the liquid but possibly the precipitation step at the  $\beta$ -surface.<sup>4</sup> The curved interface between the  $\beta$ -particle and the particles of the  $\alpha$ -matrix suggests that the local growth velocity of  $\beta$  may also be determined by the size, curvature and orientation (with respect to the  $\beta$ -surface) of the dissolving  $\alpha$ -particles close to the growth front. The liquid phase is just a solvent for reconstructive  $\alpha$ - to  $\beta$ -transformation, which occurs by breaking of  $\text{Si}_3\text{N}_4$  bonds. The existence of very thin liquid layers also seems to enhance directional grain growth,<sup>5</sup> as it is observed in this sample. The

preferred growth in the  $c$ -direction must be due to a growth favouring surface roughness of the (0001)-plane. From empirical studies<sup>1</sup> it has been suggested that this surface roughness is stabilized by a local supersaturation of the melt, due to its relatively high viscosity. Comparative investigations of the  $\alpha$ - $\beta$  interface of  $\text{Si}_3\text{N}_4$  ceramics prepared with different types and amounts of sintering aids, leading to different viscosities, should yield additional information regarding this assumption.

## Conclusion

Studies of the intermediate sintering states of  $\text{Si}_3\text{N}_4$  by investigating the microstructure of quenched samples on nm-scale by STEM may improve the understanding of the densification process and may be helpful in optimizing the microstructure with respect to the mechanical properties. The first results have been presented in this paper.

## References

1. Ziegler, G., Heinrich, J. & Wötting, G., Relationships, microstructure and properties of dense and reaction-bonded silicon nitride. *J. Mater. Sci.*, **22** (1987) 3041–86.
2. Kingery, W. D., Densification during sintering in the presence of a liquid phase. *J. Appl. Phys.*, **30** (1959) 301–10.
3. Toropov, N. A., Brazakouski, V. P., Lagim, V. V. & Kurbeva, N. N., *Phase Diagrams*, Vol. 3. Nauka, Moscow, 1972.
4. Knoch, H. & Gazza, G. E., Microstructure development in silicon nitride. In *Progress in Nitrogen Ceramics*, ed. F. L. Riley. Nato ASI Series, Martinus Nijhoff Publishers, Boston, 1983, pp. 381–92.
5. Petzow, G., Kaysser, W. A. & Amtenbrink, M., Liquid phase and activated sintering. In *Sintering—Theory and Practice*, ed. D. Kolar, S. Pejovnik & M. M. Ristic. Elsevier, Amsterdam, 1982, pp. 27–36.
6. Gazzara, C. P. & Messier, D. R., Determination of phase content of  $\text{Si}_3\text{N}_4$  by x-ray diffraction analysis. *Ceram. Bull.*, **56** (1977) 777–80.